

Characterization of Ultrafine Cellulose-filled High-Density Polyethylene Composites Prepared using Different Compounding Methods

Sevda Boran,^{a,*} Alper Kiziltas,^{b,c} Esra Erbas Kiziltas,^{b,d} and Douglas J. Gardner^b

An extensional flow mixture (EFM) system was studied, with the goal of achieving better distributive and dispersive mixing. The effects of different mixing strategies (masterbatch method (MB), polyethylene-grafted maleic anhydride (PE-g-MA) as a compatibilizer, and compounding devices, such as a single screw extruder (SSE), a twin screw extruder (TSE), and an extensional flow mixer (EFM)) on the mechanical, thermal, rheological, and morphological properties of ultrafine cellulose (UFC)-filled high-density polyethylene (HDPE) composites were investigated. Maximum tensile strength (17.7 MPa), tensile modulus (0.88 GPa), flexural strength (18.8 MPa), and flexural modulus (0.63 GPa) were obtained from the MB compounding method. The maximum stress-strain (13.8%) was obtained with EFM compounding. Polymer composites from SSE and SSE/EFM compounding methods with PE-g-MA exhibited slightly higher crystallinity compared with other compounding methods. The storage modulus of the samples prepared with the MB method was higher than those prepared with the SSE compounding method. The UFC-filled HDPE composites from the EFM compounding process exhibited lower melt viscosities than the other composites at high shear rates. Scanning electron microscopy (SEM) images showed the cellulose to be distributed and dispersed reasonably well in the HDPE matrix when using a coupling agent in combination with the MB and EFM compounding methods.

Keywords: Composites; Cellulose; Mechanical properties; Rheology; Extrusion

Contact information: a: Department of Woodworking Industry Engineering, Faculty of Technology, Karadeniz Technical University, 61830 Trabzon, Turkey; b: Advanced Structures and Composites Center, University of Maine, 04469Orono, ME; c: Department of Forest Industry Engineering, Faculty of Forestry, University of Bartın, 74100Bartın, Turkey; d: The Scientific and Technological Research Council of Turkey (Tubitak), Tunus Cad, Kavaklıdere, 06100 Ankara, Turkey;

* Corresponding author: sevdaboran@gmail.com

INTRODUCTION

In recent years, the use of renewable cellulose for polymer composites has attracted much attention as an environmentally friendly natural material. Cellulose-based micro- and nanomaterials are considered alternatives to inorganic filler-reinforced thermoplastic polymer composites for construction, automotive, and packaging applications (Yang and Gardner 2011; Endo *et al.* 2013; Abdul Khalil *et al.* 2014). These new materials can provide strong reinforcement in polymer composites (Henriksson *et al.* 2007; Ramires and Dufresne 2011). Micro- and nanocellulose has favorable features, such as renewability, biodegradability, high surface area, high modulus, high strength, and low density, in comparison to commercial fillers (*e.g.*, talc and glass fibers). Micro- and nanocellulose have been used in many applications, including reinforcement of transparent polymers, thin films of polymer electrolytes for lithium battery applications, and optoelectronic devices

(Hitoshi and Akira 2007; Khalil *et al.* 2012; Ozen *et al.* 2013; Pandey *et al.* 2013). In spite of some advantages, these renewable materials have undesired properties, such as limited thermal stability at typical melt processing temperatures of approximately 200°C, limited compatibility with many thermoplastic matrices attributable to their highly hydrophilic properties, poor dispersion characteristics in the non-polar thermoplastic melt because of strong hydrogen bonding forces between the fibers, and high moisture absorption of the fibers affecting the dimensional stability of the composite materials (Khalil *et al.* 2012; Kiziltas *et al.* 2013; Pandey *et al.* 2013).

The key challenge to uniform compounding is providing uniformly distributed and disperse mixing of fillers in polymer matrices (Rauwendaal 1998; Wang and Zloczower 2001). Composites reinforced with micro- and nanocellulose have excellent mechanical properties compared to other biomaterials, such as wood fiber and agricultural wastes (Walther *et al.* 2010; Josefsson *et al.* 2014). It has been reported that the processing method, the morphology and dimensions of the cellulose, the microstructure of the matrix, and the matrix/filler interaction all influence the mechanical properties of cellulose nanocomposites (Ramires and Dufresne 2011). It is especially important to develop methods and procedures for the uniform dispersion of micro- and nanocellulose in non-polar polymer matrices, such as polyethylene (PE), polypropylene (PP), and polylactic acid (PLA) (Balatinecz *et al.* 1999; Caulfield *et al.* 2001; Kiziltas *et al.* 2016a,b). Recently, PE-based micro- and nanocomposites have received considerable interest in electrical insulation, biomedicine, packaging, construction, furniture, aerospace, and automotive applications (Panaitescu *et al.* 2007a; Pöllänen *et al.* 2013). Previously, cellulose-based micro- and nanomaterials have been used as fillers in PE matrices (Bataille *et al.* 1990; Herrera-Franco and Aguilar-Vega 1997; Panaitescu *et al.* 2007b; Tajeddin *et al.* 2009; Shumigin *et al.* 2011; Sdrobiş *et al.* 2012; Pöllänen *et al.* 2013; Kiziltas *et al.* 2016a). The cellulose-filled PE composites are melt-mixed using a Brabender mixer, a conical twin-screw microcompounder, and a twin-screw extruder (TSE) (Shumigin *et al.* 2011; Sdrobiş *et al.* 2012; Kiziltas *et al.* 2016a). The chemical compatibility of hydrophilic cellulose and hydrophobic PE, in addition to the cellulose dispersion in PE matrices, have been improved with the addition of a coupling agent, chemical treatment of the cellulose surface, and a carrier system for cellulose-filled PE micro- and nanocomposites (Sdrobiş *et al.* 2012; Pöllänen *et al.* 2013; Kiziltas *et al.* 2016a).

Single-screw extruders (SSE), twin-screw extruders (TSE), and extensional flow mixers (EFM) are used to compound micro- and nanocomposite materials and enhance dispersion of micro- and nanoscale fillers in different polymer matrices (Li *et al.* 2007; Utracki 2007; Boran *et al.* 2016). The formulations are exposed to strong extensional flow fields in EFM. The elongational stress in EFM is generated in the gap space between the convergent-divergent (C-D) plates controlled by the geometry of the mixing cavity. These C-D plates have an adjustable gap, a hyperbolic convergence to direct the compound aggregates in the flow direction, and a divergent part to randomize the flow. The geometry of the C-D plates in EFM provides the balance of the extensional to shear stress from within the C-D plates (Li *et al.* 2007). The EFM method has the following advantages: the mixture of the two fluids is exposed to strong extensional flow fields; a series of holes are replaced by slits to decrease the pressure drop; the flow fields are occurring through a series of divergences and convergences of increasing intensity; the slit gaps are adjustable (Utracki *et al.* 2003) so that the flow can be controlled by the geometry of the mixing cavity (Nguyen and Utracki 1995; Luciani and Utracki 1996; Bourry *et al.* 1999). Currently, the most homogenous dispersion of nanofiller within the polymer matrix is usually achieved by MB

compounding, combined with SSE and EFM. Nevertheless, this approach has not been investigated for nanocellulose-reinforced thermoplastic composites.

As previously mentioned, the primary problem associated with micro- and nano-composites is their ability to obtain a homogeneous dispersion of fillers within the polymer matrix (Prashantha *et al.* 2009). The homogenous dispersion of micro- and nanoparticles is difficult within a polymer blend. The MB compounding method is a concentrated mixture of fillers encapsulated during melt compounding into a carrier resin and one of the simplest and is one of the most economical methods in processing of micro- and nanoparticles in composites. This method has been applied to overcome the shortcomings of filler homogeneity and to improve processing characteristics, physical, and mechanical properties of composites (Lee *et al.* 2008; Joo *et al.* 2011). Importantly, the dispersion of micro- and nanocellulose in MBs should be investigated and the dilution process should be carried out under appropriate processing conditions to obtain a well-dispersed micro- and nanocellulose PE matrix, as seen in multi-wall carbon nanotube nanocomposites (Prashantha *et al.* 2009). It is also necessary to understand the effects of cellulose and compatibilizers on the mechanical, thermal, and rheological properties of polymer/cellulose composites (Lee *et al.* 2008). To obtain nano/micro cellulose-based thermoplastic composites with acceptable mechanical properties, the filler dispersion within the matrix is a key criterion in non-polar polymer matrices, such as PE and PP. For example, cellulose-filled PE composites are typically melt-mixed in a Brabender mixer, conical twin-screw extruder, or SSE. Another way to enhance the dispersion of nano- and micro-fillers within the matrix is the use of SSE, TSE, and EFM, which is rather rare. Chemical compatibility between hydrophilic cellulose filler/reinforcement and hydrophobic polymer matrix, such as PE, has been improved with coupling agents or chemical treatment of the filler's surface. Improved compatibility between the matrix and the filler typically leads to better filler dispersion within the polymer matrix. Furthermore, the role of the coupling agent to improve the dispersion of cellulose in PE and its adhesion towards the polymer matrix, as well as the EFM compounding method, has yet to be thoroughly examined.

In this study, the HDPE/ultrafine cellulose (UFC) composites were produced by different compounding methods, including single-pass extrusion and MB compounding methods with or without EFM. The composites were characterized to determine their mechanical, thermal, and rheological properties.

EXPERIMENTAL

Materials

The HDPE powder was supplied in the form of polymer pellets by Equistar (Houston, Texas, USA), and PE-g-MA, the compatibilizer, was obtained from the Polybond Co. (Greensboro, North Carolina, USA). The ultrafine cellulose powder (UFC), with an average particle size of 8 μm , was supplied by J. Rettenmaier & Sohne (Rosenberg, Germany). The materials' properties are listed in Table 1. The extensional flow mixer (EFM) was attached to SSE in an attempt to obtain the best polymer mixing and dispersing. The EFM was adjusted with a gap between the C-D plates and set as $h=20 \mu\text{m}$ after pretesting.

Table 1. Material Properties

Material /Trade name	Diameter (μm)	Melt Flow Index(MFI) (g/10 min)	Density (g/cm ³)	Melting Point (MP) (°C)	Supplier
UFC/ Arboce [®] UFC 100	8	-	1.56	-	JRS
High Density Polyethylene (HDPE) /MicrotheneMP655962	300-500	5	0.95	128	Equistar
PE-g-MA/ Polybond [®] 3029	-	4	0.96	130	Polybond

*PE-g-MA: Polyethylene-grafted maleic anhydride

Methods

Masterbatch(MB)method

The HDPE and UFC had an initial moisture content (MC) of approximately 6%. The HDPE and UFC were dried for a minimum of 16 h until they reached below 1% MC in an oven at 80 °C. All moisture measurements were performed according to the ASTM D 5229 M14 (2014) testing standard. First, the HDPE powder was mixed with the UFC by thermal compounding using a C.W. Brabender Prep-mixer[®] (South Hackensack, NJ, USA) with a bowl mixer to obtain a MB containing 10% UFC. The mixer temperature was set at 160 to 170 °C, with a melting temperature of 170 to 180 °C, and a rotor speed of 60 rpm. The procedure for the MB compounding method was as follows: the reaction chamber was heated to 180 °C and the mixer was set at 60 rpm; then, the HDPE powder was fed into the chamber; the HDPE powder was completely melted after 5 min; the UFC was slowly added to the HDPE melt; the system was kept closed for 5 min; after the thermal mixer was stopped, the blending material obtained was removed from the mixing system.

In the second step, the MB was diluted to 4 wt.% UFC. The dilution was performed using a SSE (Davis-Standard, Pawcatuck, North America, USA) or a SSE/EFM. Based on our preliminary results, the EFM was adjusted with the gap between the C-D plates at $h=20$ μm. The PE-g-MA was premixed with other materials before the extrusion process. The extrudate was solidified directly in an air-cooling system after the SSE or SSE/EFM process while being pulled with a 2201 Series End Drive Conveyor from Dorner MFG Corp. (Hartland, WI, USA). The solidified extrudate was pelletized using a pelletizer for the laboratory extrusion runs from C.W. Brabender Instruments, Inc. (South Hackensack, New Jersey, USA). The processing parameters for the MB compounding method are shown in Table 2.

Single pass method

The UFC and PE-g-MA were dried in an oven at 80°C overnight before melt compounding. The HDPE powder, PE-g-MA, and UFC were premixed concurrently, placed in the extruder feed hopper, and then into a speed mixer. The sample was extruded at 60 rpm using a C.W. Brabender 20 mm clamshell segmented twin screw extruder, attached to the Intelli-Torque Plastic-Corder drive system (C. W. Brabender Instruments, (South Hackensack, New Jersey, USA)) for TSE and the screw configuration of the system was the stand-alone TSE20/40D version. The same pelletizer and cooling systems were used. The processing parameters are shown in Table 2.

Table 2. (a) Temperature (°C) Profile for the SSE, TSE, and EFM; (b) Processing Conditions used in Injection Molding, SSE, and TSE Compounding

a) Single-screw extruder(SSE)						
Zones	Z-1	Z-2	Z-3	Z-4	Clamp	Die
Temp. (°C)	145	145	150	150	160	170
a) Twin-screw extruder(TSE)						
Zones	Z-1	Z-2	Z-3	Z-4	Z-5	Die
Temp. (°C)	145	145	150	150	160	170
a) Extensional flow mixer(EFM)						
Zones	Z-1	Z-2	Z-3			
Temp. (°C)	190	200	200			
b) Process parameters						
Twin screw speed (rpm)			60			
Single screw speed (rpm)			50			
Injection pressure (MPa)			17			
Holding time (s)			10			
Cooling time (s)			10			
Injection mold temperature (°C)			180			
Injection barrel temperature (°C)			180			

Table 3 shows the composition and designation of UFC-filled HDPE polymer composites. The SSE, SSE/EFM, and TSE samples are also symbolized as S, E, and T, respectively (Table 3). The weight ratio of UFC to PE-g-MA was held constant at 1:2 throughout this study, based on the preliminary findings. For mechanical testing, the pelletized samples were dried at 80 °C overnight before being injection molded. All samples were injection molded using a barrel temperature of 180 °C, mold temperature of 180 °C, and injection pressure of 17 MPa.

Table 3. Composition and Designation of UFC-filled PE Polymer Composites

Sample Designation	High Density Polyethylene (HDPE)	Polyethylene graft maleic anhydride (PE-g-MA) (wt.%)	Ultrafine cellulose (UFC) (wt.%)	Processing method
S	100	-	-	SSE
S/E	100	-	-	SSE/EFM
C/S	96	4	-	SSE
UFC/S	96	-	4	SSE
UFC/T	96	-	4	TSE
UFC/S/E	96	-	4	SSE/EFM
UFC/S/MB	96	-	4	SSE/MB
UFC/S/E/MB	96	-	4	SSE/EFM/MB
UFC/C/S	88	8	4	SSE
UFC/C/S/E	88	8	4	SSE/EFM
UFC/C/S/MB	88	8	4	SS/MB
UFC/C/S/MB/E	88	8	4	SSE/MB/EFM

SSE: Single-screw extruder; TSE: Twin-screw extruder; EFM; Extensional flow mixer; UFC: Ultrafine cellulose; MB: Masterbatch; C: Coupling agent

Mechanical Tests

All the mechanical tests were carried out in an environmentally controlled room at 23 ± 2 °C and $50 \pm 5\%$ relative humidity.

Tension testing

The tensile tests were performed using an Instron 5966 (Norwood, MA, USA) with a 10-kN load cell at a crosshead speed of 5 mm/min, according to ASTM D638-10 (2010). The dimensions of specimens were selected as 5x13x165 mm. The elongation of the tested specimen was determined with an extensometer. The modulus was determined according to the slope. The tensile strength was determined as the maximum load divided by the initial cross-sectional area. A minimum of six samples were tested for each composition, coupled with the relevant processing method, and the samples were pooled.

Flexural testing

Flexural tests of the samples were performed according to ASTM D790-10 (2010). The flexural tests were conducted using an Instron 8872 (Norwood, MA, USA) with a 1-kN load cell. The size of samples was 5 mm x 13 mm x 120 mm. The support span was 50 mm. The sample was placed on two supporting pins and set a specified distance apart. The test was stopped when the specimen broke before 5%. All of the samples were tested at a loading rate of 1.25 mm/min. At least six specimens were tested for each composition. The flexure test results are depicted as the mean of all tested samples.

Izod impact test

The notched Izod impact tests according to ASTM D256 (2010) were carried out using a Resil 50 B impact testing machine (Ceast®, Akron, Ohio, USA). The specimens were prepared at 5 mm x 13 mm x 65 mm. These specimens were clamped to the bottom of the test fixture. The hammer of this test machine was 2.75 J, and this hammer was released from a specified height. The depth under the sample width and the notch were entered before the machine recorded the energy required to break the test sample. A minimum of 10 samples were tested from each composition and the test results were reported the mean of all of the tested samples.

Differential scanning calorimetry (DSC)

Differential scanning calorimetry was performed on a TA Q2000 (TA Instruments, New Castle, USA) analyzer, and a sample weight of 8 to 10 mg was used to measure the thermal transitions of composites, including the crystallization temperature (T_c), melting temperatures (T_m), and enthalpy of transitions (ΔH). The samples were equilibrated at 25 °C for 5 min, and then heated at a rate of 20 °C/min to 200 °C. Then, the samples were held for 5 min to erase thermal history, and cooled at a rate of 10 °C/min to 0 °C. Next, the samples were held for 5 min and heated at a rate of 10 °C/min to 200 °C. All of these procedures were performed under a nitrogen atmosphere. The melting temperatures (T_m) were determined from a second scan, and T_m was recorded as the peak temperature of the melting endotherm.

The ‘all samples’ crystallinity (X_c) index, which is an indication of the amount of crystalline region in the polymer with respect to amorphous content, was calculated as follows (Kiziltas *et al.* 2013),

$$X_c = \frac{\Delta H_f \times 100}{\Delta H_f^\circ \times \omega} \quad (1)$$

where ΔH_f is the heat of fusion of the neat HDPE and composites, ΔH_f° is the heat of fusion for 100% crystalline HDPE ($\Delta H_{100}^\circ=287.3$ J/g), and ω is the mass fraction for HDPE in the composites (Mirabella and Bafna 2002). The results were calculated as the mean of three samples.

Rheology

Rheological properties of the composites were measured by a stress-controlled Bohlin Gemini rheometer (Aimil Ltd., New Delhi, USA) with a parallel plate fixture (25 mm diameter) at a temperature of 180 °C. The gap between the two parallel plates was maintained at 2 mm to calculate the storage moduli (G'). All of the samples were set between the parallel plates after loading. The rheological measurements were used to determine the dynamic complex viscosity ($|\eta|^*$), the storage and loss moduli (G' and G''), and the loss factor ($\tan \delta$) to evaluate of the rheology properties of the samples. A strain of 1% was used to ensure all measurements were tested within the linear viscoelastic range for each sample (Kiziltas *et al.* 2013).

Scanning electron microscopy (SEM)

Scanning electron micrographs were used to assess the degree of cellulose dispersion within the PE matrix. Test specimens were immersed in liquid nitrogen and fractured. The fractured surfaces were gold sputtered and inspected on a ZEISS EVO LS 10 (North Chesterfield, VA, USA) scanning electron microscope. The SEM images were recorded at 10 kV using 2000X magnification.

Statistical analysis

Differences among treatment groups were analyzed using one-way analysis of variance (ANOVA) and the means were separated using the Tukey-Kramer (HSD) method of pair wise comparison if the overall ANOVA model was significant ($P<0.05$) (JMP Statistical Discovery Software Version 8).

RESULTS AND DISCUSSION

Mechanical Properties

Table 4 indicates the mechanical properties of the neat HDPE- and UFC-filled HDPE composites. UFC/C/S/MB method resulted in a maximum tensile strength of 17.7 MPa. The tensile strength of the samples ranged from 15.3 MPa to 17.7 MPa. When the coupling agent was introduced, the tensile strength for all of the compounding methods improved considerably. It is known that coupling agent strengthens cellulose-based polymer composites and decreases the moisture absorption of cellulose fibers (Botros 2003). The effect of PE-g-MA on the mechanical properties of microcrystalline cellulose and viscose fibers was also studied by Pöllänen *et al.* (2013). They found that PE-g-MA increased the tensile strength by increasing the adhesion between the filler and the HDPE matrix, based on SEM results (Pöllänen *et al.* 2013). Tokihisa *et al.* (2006) declared that it was unclear why the SSE/EFM compounding method increased performance because of better dispersion compared with the TSE/EFM compounding method. It is known that better dispersion was obtained under mild compounding conditions (Dennis *et al.* 2001; Tokihisa *et al.* 2006).

Table 4. Mechanical Properties of the Neat HDPE- and UFC-filled HDPE Composites

Samples	Tensile properties			Flexural properties		I.S. (J/m)
	ϵ (%)	σ_t (MPa)	E_t (GPa)	E_f (GPa)	σ_f (MPa)	
S	13.4 (bc) (0.5)	16.3 (d) (0.5)	0.78(abcd) (0.07)	0.51 (de) (0.02)	15.7 (f) (0.4)	127.4 (b) (11.1)
S/E	15.3 (a) (0.5)	15.7 (e) (0.3)	0.72 (cd) (0.05)	0.53 (d) (0.02)	16.0 (ef) (0.2)	155.5 (a) (15.2)
C/S	12.0 (ef) (0.4)	17.1 (bc) (0.2)	0.84 (ab) (0.09)	0.53 (d) (0.01)	16.1 (ef) (0.3)	140.2 (b) (12.7)
UFC/S	13.3 (bcd) (0.3)	15.5 (e) (0.1)	0.75 (bcd) (0.03)	0.50 (e) (0.01)	15.5 (f) (0.3)	68.7 (c) (5.7)
UFC/T	13.7 (b) (0.2)	15.8 (de) (0.3)	0.78 (abcd) (0.04)	0.57 (c) (0.01)	17.2 (cd) (0.1)	70.5 (c) (2.8)
UFC/S/E	13.8 (b) (0.3)	15.9 (de) (0.3)	0.83 (ab) (0.04)	0.61 (ab) (0.01)	17.8 (abcd) (0.2)	59.8 (cd) (2.9)
UFC/S/MB	13.2 (bcd) (0.5)	15.5 (e) (0.1)	0.82 (abc) (0.05)	0.53 (d) (0.02)	16.7 (de) (0.2)	62.9 (c) (6.3)
UFC/S/MB/E	13.3 (bcd) (0.7)	15.6 (e) (0.2)	0.81(abc) (0.05)	0.59 (bc) (0.01)	17.8 (abc) (0.1)	60.6 (cd) (3.1)
UFC/C/S	12.7 (cde) (0.4)	17.3 (ab) (0.2)	0.69 (d) (0.02)	0.58 (bc) (0.01)	17.8 (bc) (0.2)	63.4 (c) (5.7)
UFC/C/S/E	11.9 (ef) (0.2)	17.2 (bc) (0.1)	0.87 (a) (0.02)	0.59 (bc) (0.01)	17.3 (cd) (0.3)	71.4 (c) (4.6)
UFC/C/S/MB	11.5 (f) (0.5)	17.7 (a) (0.3)	0.75 (bcd) (0.05)	0.63 (a) (0.01)	18.8 (a) (0.2)	49.8 (d) (4.6)
UFC/C/S/MB/E	12.6 (de) (0.4)	16.8 (c) (0.2)	0.88 (a) (0.04)	0.61(ab) (0.02)	18.4 (ab) (0.1)	50.1 (d) (4.8)

*The values in the parentheses are standard deviations

**Means with the same letter for each property were not significantly different at the 5% significance level

ϵ : Strain at the maximum stress

The addition of the coupling agent to the EFM compounding method resulted in a better tensile modulus than the UFC/C/S and UFC/C/S/MB compounding methods. The EFM attachment to the SSE provided a better tensile modulus than the UFC/S compounding method. Combining SSE and MB demonstrated a minor improvement in the tensile modulus over the MB only method. It has been reported that clay-containing polymeric nanocomposites using SSE/EFM compounding resulted in better dispersion and mechanical performance compared with TSE (Utracki 2007). Some researchers have reported that using a MB compounding method results in better material property through precise control of filler concentration in terms of mechanical properties. The MB compounding method ensures better dispersive mixing, more uniform exfoliated structure, and less reduction of the deformation properties compared with direct compounding

(Lopez-Quintanilla *et al.* 2005; Li *et al.* 2007; Treece *et al.* 2007; Etelaaho *et al.* 2009). Masterbatch compounding with cellulose nanocrystal (CNC)/polycarbonate (PC), CNC/acrylonitrile-butadiene-styrene (ABS), and microcrystalline cellulose (MCC)/PP have been prepared in previous studies (Spoljaric *et al.* 2009; Ma *et al.* 2015; Mariano *et al.* 2015). Nevertheless, the UFC/S/MB/E compounding method produced a lower tensile modulus than the UFC/S/E compounding method. There is limited information regarding MB dilution on the mechanical properties of polymer composites using ultrafine cellulose. However, it is known that cellulose acts as a mechanical reinforcement of the polymer. When a composite is filled with cellulose, the tensile modulus of the polymer composite improves considerably (Mathew *et al.* 2005; Petersson and Oksman 2006; Kiziltas *et al.* 2010). Polymer composites can be affected by filler dispersion and size of the cellulose fiber particles in the polymer matrix. It is known that the reinforcing ability of cellulose micro- and nanoparticles results from their high surface area and good mechanical properties; however, cellulose micro- and nanoparticles should be well-dispersed in the polymer matrix to achieve notable increases in mechanical properties. Their small size does not generate large stress concentrations in the polymer matrix, so well-dispersed cellulose particles can improve tensile properties (Kvien *et al.* 2005; Kvien and Oksman 2007; Yang *et al.* 2011). Further evidence on the agglomeration and dispersion of UFC samples with MB and EFM compounding into the polymer matrix will also be discussed in the next SEM analysis section. Microscopic observation also showed that the cellulose was well distributed and dispersed in the HDPE matrix when using a coupling agent and the MB or EFM compounding methods. Therefore, the addition of MB or EFM to the compounding method can be advised.

Table 4 illustrates the strain at the maximum stress change in UFC-filled HDPE composites using SSE, TSE, SSE/EFM, SSE/MB, SSE/MB/EFM, and each of these compounding methods included the addition of a coupling agent, excluding TSE. The maximum value for strain at the maximum stress was achieved from the S/E compounding method, while the minimum value was observed from the UFC/C/S/MB with the coupling agent. The highest value for strain at the maximum stress was 13.8%. When compared to the MB compounding method, the UFC/S/MB/EFM without the coupling agent produced the maximum strain value. All samples produced with the coupling agent exhibited lower strain at the maximum stress than the compounding methods without the coupling agent because of the enhanced adhesion between the UFC and the HDPE matrix. Similar results were reported by Shao *et al.* (2015) and Ismail *et al.* (2001) for triethoxysilane (AS), methacryloxy propyl trimethoxy silane (MS), and maleic anhydride-grafted polypropylene (MAPP)-treated natural fiber (cellulose, sawdust, and wheat straw), and reinforced PP and silane-treated white rice husk ash-filled PP/natural rubber composites, respectively (Ismail *et al.* 2001; Shao *et al.* 2015). Shao *et al.* (2015) explained that better adhesion yields more restriction of deformation capacity of composites; therefore, catastrophic failure occurs after small strain deformations. The highest values of strain at the maximum stress for all combinations of EFM compounding were obtained from the UFC/S/E compounding method without the coupling agent. The elongational flow in EFM provides excellent mixing, decreased viscous dissipation and lower melt temperatures, dispersed at large viscosity ratios, and enhanced distributive mixing. The SSE exhibited poor dispersive mixing capability compared with TSE.

There are two important differences between TSE and SSE in terms of the mixing mechanism. The flow in high-stress regions (HSR) of most mixers is predominantly shear flow and the fluid elements pass through the HSR only once in SSE compounding. In TSE

compounding, the flow in the kneading disks has a strong elongational flow and the fluid elements pass through the HSR several times (Rauwendaal *et al.* 1999). However, the use of EFM shows that the mixture of two compounds is exposed to strong extensional flow fields because the flow fields are generated by a series of convergences and divergences (Nguyen and Utracki 1995; Utracki 2003). The EFM compounding method has some advantages for distributive and dispersive mixing. Distributive mixing in EFM compounding is more efficient because the interfacial area is much higher than in the shear flow. Consequently, dispersive mixing is also much higher than that of shear because the drop deformability in elongation is several times higher than in shear (Tokihisa *et al.* 2006). Some researchers also reported favorable mechanical properties in a well-dispersed nanocomposite with cellulose nanofibrils (Walther *et al.* 2010; Josefsson *et al.* 2014).

The best flexural strength and flexural modulus values were obtained from the UFC/C/S/MB compounding method. Flexural strength values ranged from 15.5 to 18.8 MPa, while the flexural modulus ranged from 0.50 to 0.63 GPa. It was obvious that the EFM compounding method improved the flexural properties of the ultrafine cellulose-filled composites compared to UFC/T, UFC/S, and UFC/S/MB compounding methods. Using the MB compounding method had a beneficial role in improving the flexural strength. The addition of the coupling agent to UFC/S and UFC/S/MB compounding methods resulted in better flexural properties. Li *et al.* (2007) studied the effects of mixing strategies (with or without MB compounding method), and processing devices (TSE, SSE, and SSE/EFM) for PP-based clay nanocomposites. As a result, the flexural properties of the samples prepared from MB compounding were better than those from the single-pass method (Li *et al.* 2007).

As shown in Table 4, the maximum value for the impact strength was obtained from the UFC/C/S/E compounding method. When using EFM compounding without the coupling agent, the impact strength decreased slightly. However, it is noteworthy to mention that using the coupling agent had less of an impact on the strength value in comparison with UFC/S, UFC/S/MB, UFC/S/MB/E compounding methods. The results also indicated that using the MB compounding method produced lower impact strength values than the UFC-filled HDPE composites prepared from different compounding methods, excluding the UFC/S/MB/E method. Similar results were also reported by Li and Chen (2007) for HDPE/expanded graphite nanocomposites prepared *via* MB compounding. The lower impact strength can be explained by the lower interaction made by MB than the other UFC-filled HDPE composites prepared by different compounding methods (Li and Chen 2007).

Differential Scanning Calorimetry Analysis

Differential scanning calorimetry measurements were used to characterize the thermal properties of UFC-filled HDPE composites prepared by various compounding methods. Melting and crystallization temperatures of the specimens did not notably affect the outcomes. Šumigin *et al.* (2012) declared that crystallization and melting temperatures of the low density polyethylene (LDPE) and LDPE with cellulose do not change with cellulose content. Table 5 shows that the crystallization temperatures were between 116 and 118 °C, while the melting temperatures were approximately 129 °C. Using of the MB compounding method resulted in a small decrease in the melting and crystallization enthalpy for all of the polymer composites. The DSC results showed that the addition of the coupling agent influenced the HDPE melting and crystallization enthalpies for UFC/S and UFC/S/E compounding methods. Araujo *et al.* (2008) also found that the coupling

agent affected the melting and crystallization behavior of natural fiber-reinforced PE composites. The degree of crystallinity of all composites was also calculated in Table 5. There was a minor reduction in the degree of crystallinity for the MB compounding methods. The UFC/S and UFC/C/S/E methods exhibited a slightly higher degree of crystallinity compared to the other compounding methods.

Table 5. Melting and Crystallization Parameters of the Neat HDPE and UFC-Filled Composites

Samples	Melting temperature (T_m) (°C)	Crystallization temperature (T_c) (°C)	Enthalpy of melting (ΔH_m) (J/g)	Enthalpy of crystallization (ΔH_c) (J/g)	Crystallinity (X_c) (%)
S	130.1 (0.3)	116.4 (0.4)	181.4 (1.9)	182.5 (2.4)	65.5 (1.7)
S/E	129.7 (0.1)	116.1 (0.1)	180.6 (2.2)	180.7 (1.6)	65.2 (2.2)
C/S	129.9 (0.1)	116.8 (0.3)	182.8 (3.2)	181.6 (3.1)	66.0 (4.2)
UFC/S	129.2 (0.2)	117.0 (0.2)	178.8 (1.4)	178.8 (1.1)	67.2 (1.4)
UFC/T	129.6 (0.0)	115.8 (0.2)	176.0 (3.5)	175.2 (3.4)	66.2 (3.5)
UFC/S/E	129.8 (0.0)	116.6 (0.4)	173.5 (0.0)	175.6 (0.0)	65.2 (3.5)
UFC/S/MB	129.5 (0.1)	116.7 (0.2)	172.6 (3.2)	171.9 (3.0)	64.9 (3.3)
UFC/S/MB/E	129.6 (0.2)	118.6 (1.5)	169.8 (0.6)	170.7 (2.0)	63.8 (4.9)
UFC/C/S	129.5 (0.2)	117.6 (0.4)	180.3 (4.9)	183.5 (1.9)	67.8 (3.5)
UFC/C/S/E	129.9 (0.2)	117.4 (0.5)	179.0 (3.5)	181.4 (1.8)	67.3 (3.5)
UFC/C/S/MB	129.7 (0.4)	116.8 (0.4)	168.3 (2.8)	168.7 (2.3)	63.3 (2.8)
UFC/C/S/MB/E	129.3 (0.1)	118.1 (0.1)	169.8 (1.1)	171.6 (1.3)	63.9 (1.1)

*Parentheses indicate standard deviation.

Rheological Properties

The storage moduli (G' at 170°C as a function of frequency (ω)) of composites prepared by single-pass (SP) extrusion (a), compatibilized (b), and MB compounding (c) methods are shown in Fig.1. The S and S/E exhibited typical melt behavior in the thermal region; the storage modulus (G') increased with the shear frequency in Fig.1a. The addition of UFC increased the G' of the composites, especially in the thermal region for UFC/S, UFC/T and UFC/S/E, which was attributed to the strong cellulose-cellulose particle interaction. The difference in the storage modulus between composites and neat polymers (S and S/E) was less distinguishable with increasing frequency because the cellulose particles were disconnected and the cellulose-cellulose interactions were weaker (Volk *et al.* 2015). The samples prepared using the SP method (Fig. 1a) in UFC/S/E composites exhibited a larger G' , while those from TSE and SSE were smaller. The relative magnitude changes of G' for the UFC/S/E compounding method indicated that the composite was

dominantly more elastic when the UFC was processed with EFM. Figure 1b shows that all of the filled systems, with or without the coupling agent, had a higher G' than the neat HDPE. It was also observed that the coupling agent did not improve the G' of the composites as compared to the composites from SSE (UFC/S) without the coupling agent. Furthermore, the G' values of samples prepared by the MB compounding method (Fig. 1c) were higher to those prepared by the SP compounding method. These results indicated that preparation of cellulose composites from MB obtained a well-dispersed cellulose and increase melt elasticity (Prashantha *et al.* 2009).

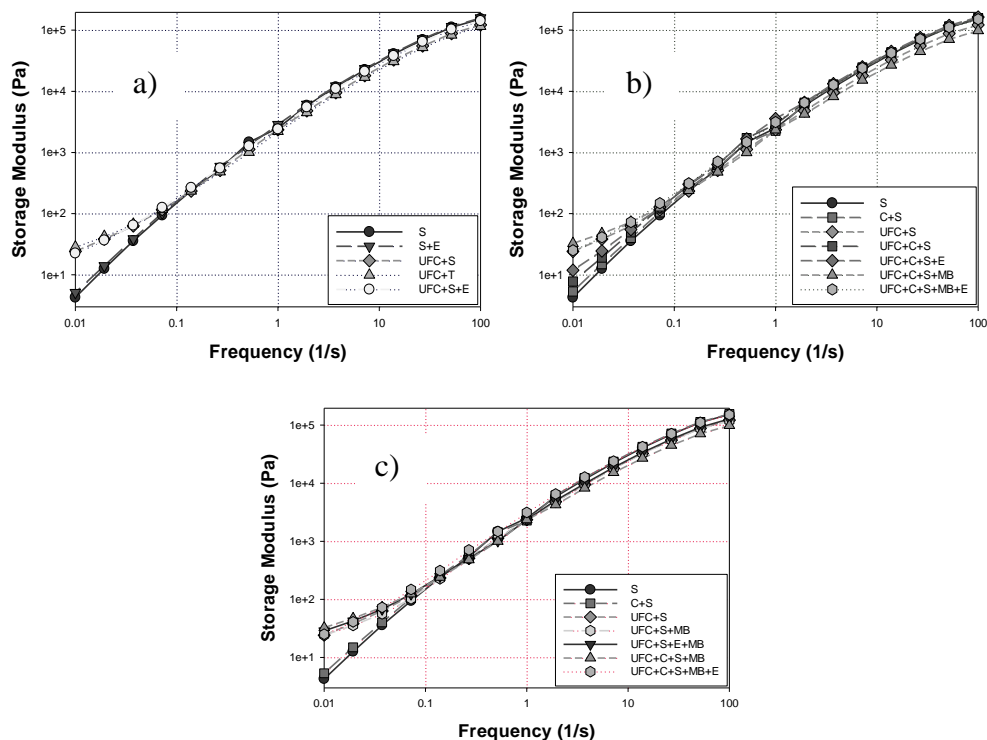


Fig. 1. Storage modulus G' at 170 °C for as a function of frequency for a) single pass compounding, b) compatibilized systems, and c) MB compounding

The complex viscosity (η^*) of the neat HDPE and the UFC-filled HDPE composites measured at 170 °C as a function of frequency (ω) is shown in Fig. 2. The complex viscosities decreased with an increase in ω , indicating shear thinning behavior and pseudoplastic characteristics of HDPE and the UFC-filled HDPE composites. It was observed from Fig. 2a that the composites from the SSE (UFC/S) and TSE (UFC/T) extruders, without the coupling agent, exhibited a reduced shear thinning behavior compared to the neat HDPE. This reduction in complex viscosity for UFC/S and UFC/T could have been a result of decreased polymer molecular entanglement density, causing a small disruption in the polymer chain entanglement network (Hatzikiriakos *et al.* 2005). This observation was in agreement with Mukherjee *et al.* (2013) for microcrystalline-filled PLA composites. It was also observed that η^* was neither similar nor lower than the neat HDPE for composites, including those with the coupling agent (Fig. 2b) and processed with MB methods (Fig. 2c).

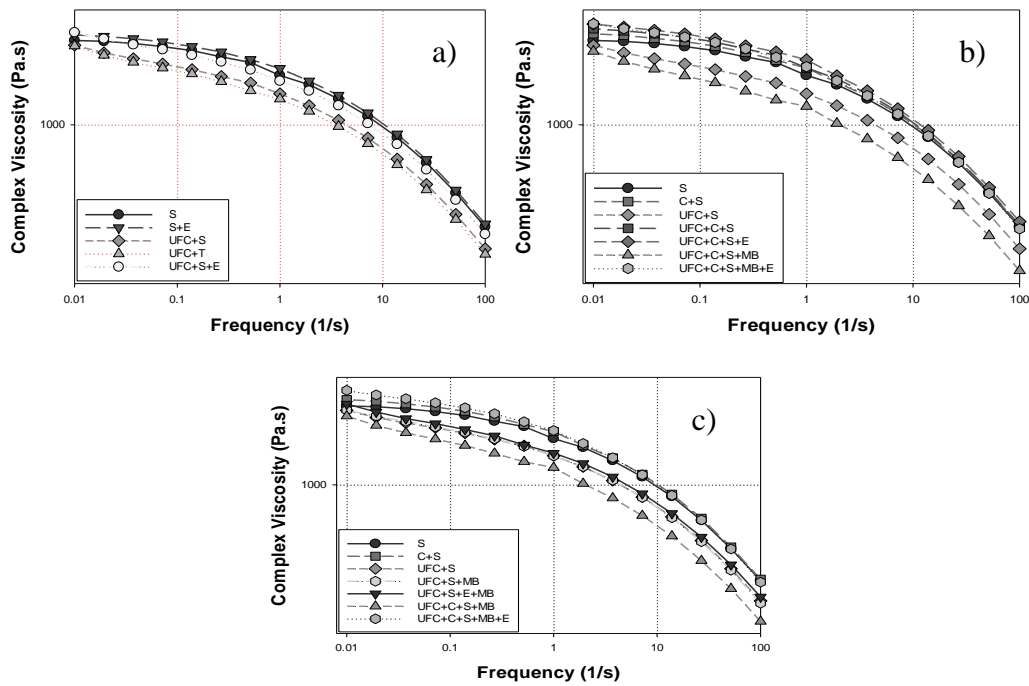


Fig. 2. The complex viscosity of the samples as a function of frequency for a) single pass compounding, b) compatibilized systems, and c) MB compounding

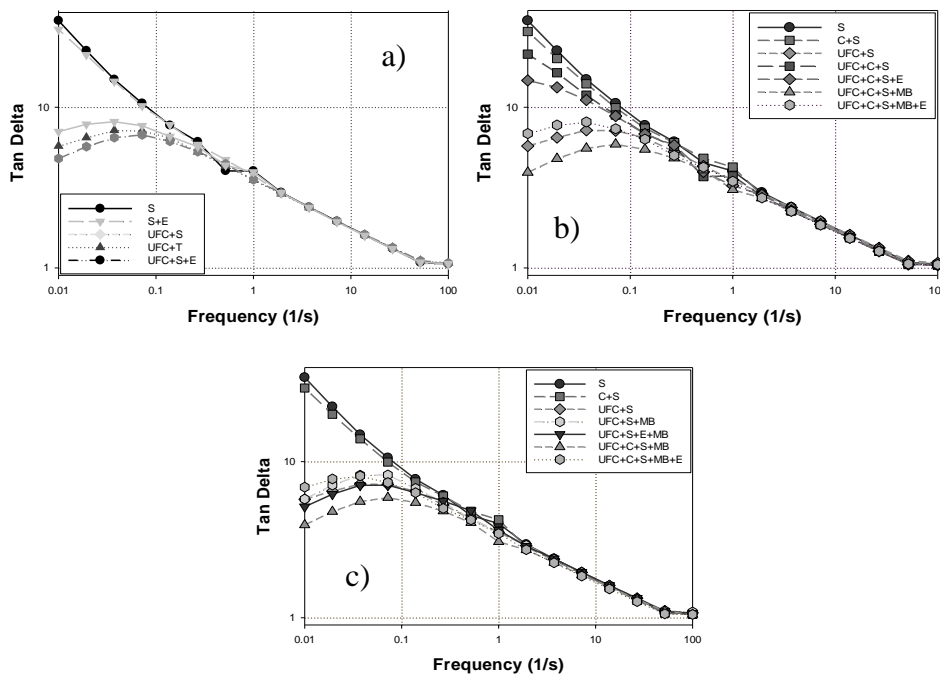


Fig. 3. The tan delta of the samples as a function of frequency for a) single pass compounding, b) compatibilized systems, and c) MB compounding

Damping characteristics ($\tan \delta = \text{loss modulus } (G'')/\text{storage modulus } (G')$) of the UFC-filled HDPE composites were also investigated, and Fig.3 shows the variation in $\tan \delta$ according to the frequency. It was evident that at lower frequencies the $\tan \delta$ decreased with the incorporation of UFC, which was mainly attributed to the existence of effective interfacial bonding between the UFC and HDPE matrix. Thus, the viscoelastic

energy dissipation in the composite was limited (Lozano *et al.* 2004). It was also observed that the UFC-filled HDPE composites processed with EFM compounding exhibited a lower tan delta compared to the other composites (Fig. 3c). This implies that the composites from EFM compounding became substantially less viscous and dissipated less energy during shear deformation compared to the other composites (Ten *et al.* 2012).

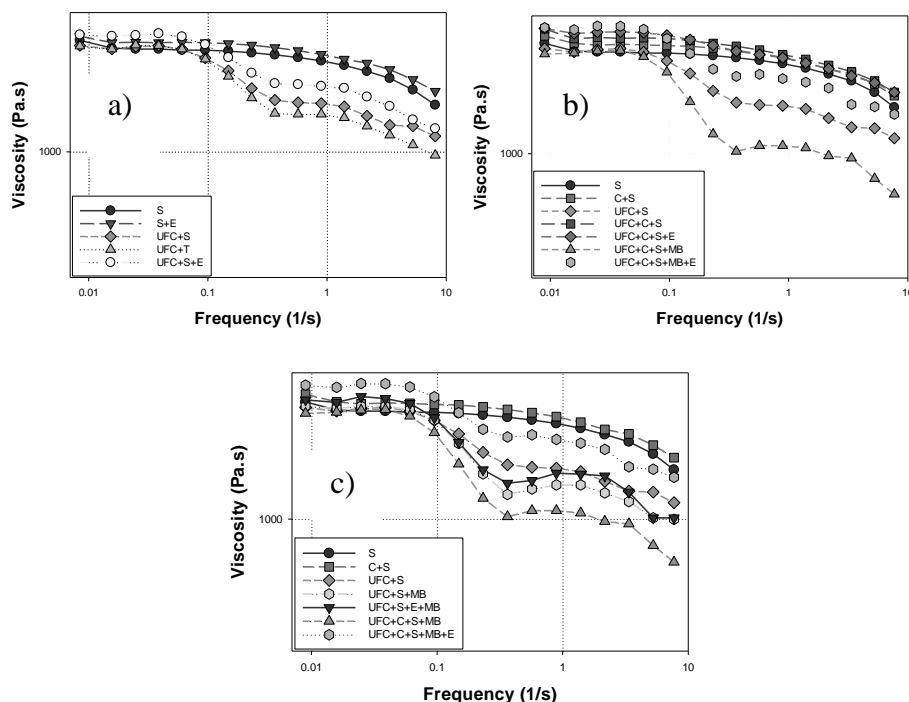


Fig. 4. Steady shear viscosity of the samples as a function of shear rate for a) single pass compounding, b) compatibilized systems, and c) MB compounding

Figure 4 shows the apparent viscosity as a function of shear rate at 170 °C for the neat HDPE and its composites. It was observed that the curves exhibited the characteristics of typical pseudoplastic materials, and the viscosity of the composites decreased with increasing shear rate. It is known that the viscous stress predominates over particle interactions; thus, the alignment is greater and the viscosity lessens at higher shear rates (Yu *et al.* 1993). In general, the UFC-filled HDPE composites exhibited higher viscosities than the neat HDPE at lower shear rates (< 0.1 1/s). Chafidz *et al.* (2014) discovered a similar phenomenon that was attributed to the restriction of molecular mobility and the reduction in free volume induced by the interaction and dispersion of cellulose in the polypropylene matrix. Similar to the storage modulus, the samples prepared using the SP compounding method (Fig. 4a) in UFC/S/E composites exhibited a larger melt viscosity, while those from TSE and SSE were smaller. Owing to the improved UFC-HDPE interfacial adhesion, the viscosity of the UFC-filled HDPE composites was either higher or comparable with the addition of coupling agent (Fig. 4b) at all shear rates except for UFC/C/S/MB in comparison with UFC/S. The effect of MB compounding on the viscosity of UFC-filled HDPE composites is unclear (Fig. 4c). Overall, the UFC-filled HDPE composites from the EFM compounding process showed a lower melt viscosity compared with the other composites at high shear rates. It was unclear what mechanism was responsible for the reduction in the melt viscosity of the composites at higher shear rates. Possible reasons are the slip between the HDPE and UFC during high shear flow or a

reduced molecular weight of the HDPE because of the degradation in the presence of UFC in EFM process. More detailed studies, including rheological studies (capillary rheometer) and polymer molecular weight characterization, will be required to understand the effect of the EFM process on the rheological properties (low and high shear rate effect on the viscosity) of composites (Cho and Paul 2001).

Scanning Electron Microscopy Analysis

The SEM images of HDPE composites prepared by UFC are shown in Figs. 5 and 6. It was observed from Fig. 5a that individual large particles were dispersed throughout the polymer matrix. Figures 5b, 5c, 5d, and 5e show the SEM images for the UFC/T, UFC/S/E, UFC/S/MB, UFC/S/E/MB compounding methods, respectively. Some agglomerates separated individual particles and showed better dispersion between the polymer matrix and UFC, compared with SSE and TSE compounding method. The effect of the coupling agent was observed in Figs. 6a, 6b, 6c, and 6d. These SEM images show that using PE-g-MA resulted in better dispersion as discussed previously in the tensile properties. The reason for improved tensile strength and better dispersion can be explained by the interaction between the maleic anhydride group, PE-g-MA, and the hydroxyl group of cellulose through ester and/or hydrogen bonding. Enhanced adhesion and better dispersion have also been reported by Paunikallio *et al.* (2003) and Pöllänen *et al.* (2013) for viscose fiber and MCC-filled PE and viscose fiber-filled PP composites in the presence of a coupling agent, respectively.

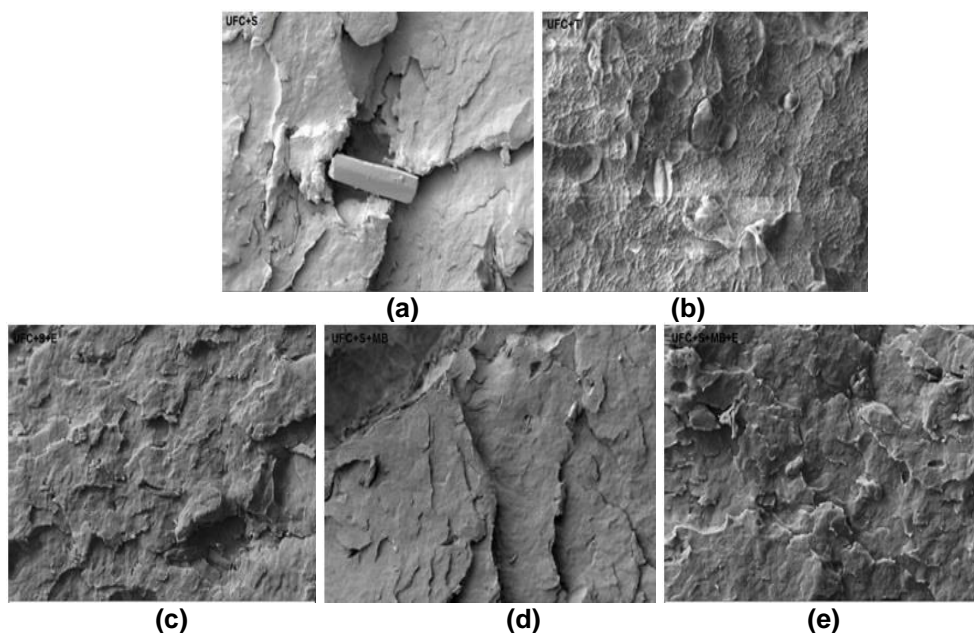


Fig. 5. Scanning electron micrographs of UFC-filled HDPE composites for a) UFC+S, b) UFC+T, c) UFC+S+E, d) UFC+S+MB, and e) UFC+S+MB+E compounding methods without the coupling agent

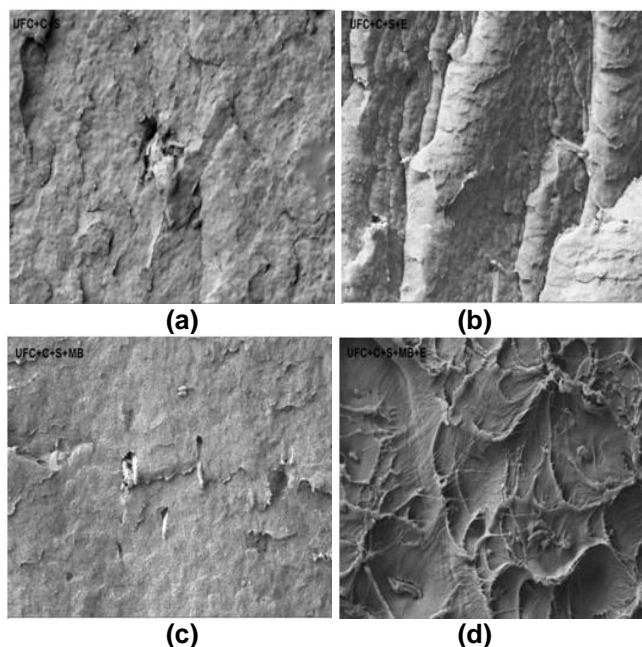


Fig. 6. Scanning electron micrographs of UFC-filled HDPE composites for a) UFC+C+S, b) UFC+C+S+E, c) UFC+C+S+MB, and d) UFC+C+S+MB+E compounding with the coupling agent

CONCLUSIONS

1. The tensile strength values of the EFM and the coupling agent were higher than those of the other composites because using a coupling agent with cellulose polymer composites strengthened the composite. The maximum tensile modulus of elasticity (0.88 GPa) was obtained using the UFC/C/S/MB/E compounding method. Similar to impact strength, S+E method without PE-g-MA gave better strain at maximum stress value. The addition PE-g-MA resulted in better tensile strength. But adding of PE-g-MA for SSE and S+MB method led a decrease of tensile modulus of elasticity value.
2. When comparing flexural properties, the MB compounding method exhibited an improvement in the flexural strength and the flexural modulus when using PE-g-MA.
3. The DSC observations showed that the addition of cellulose decreased the melting and crystallization enthalpies of the composites. The melting and crystallization enthalpies of UFC/S and UFC/S/E methods increased upon the addition of PE-g-MA.
4. Similar to the storage modulus, the samples prepared using the SP compounding method in the UFC/S/E composites exhibited greater melt viscosities than composites from TSE and SSE compounding. The EFM compounding demonstrated a lower tan delta compared to the other composites. Overall, the UFC-filled HDPE composites from the EFM compounding method exhibited a lower melt viscosity in comparison with the other composites at higher shear rates.
5. Based on the SEM imaging, particles dispersed completely into the polymer matrix in the UFC/S compounding method. Using PE-g-MA provided better dispersion for compounding methods.

6. It can be concluded from SEM and mechanical results that the EFM device and MB compounding methods can be successfully employed to provide better mixing, compounding, and dispersement of cellulose into HDPE matrices.

ACKNOWLEDGMENTS

The authors thank Maine Agricultural and Forest Experiment Station (MAFES) project ME09615-08MS and the Wood Utilization Research Hatch project for funding. The Council of Higher Education (YOK) and Karadeniz Technical University have been acknowledged for the scholarship of the postdoctoral researcher Sevda Boran to do this study at the University of Maine. The authors would like to thank Alex Nash and Chris West for the sample preparation and characterization. This is the 3495th paper of the Maine Agricultural and Forest Experiment Station.

REFERENCES CITED

- Abdul Khalil, H. P. S., Davoudpour, Y., Nazrul Islam, M., Mustapha, A., Sudesh, K., Dungani, R., and Jawaid, M. (2014). "Production and modification of nanofibrillated cellulose using various mechanical process: A review," *Carbohydrate Polymers* 99, 649-665. DOI: 10.1016/j.carbpol.2013.08.069
- Araujo, J. R., Waldman, W. R., and de Paoli, M. A. (2008). "Thermal properties of high density polyethylene composites with natural fibres: Coupling agent effect," *Polymer Degradation and Stability* 93(10), 1770-1775. DOI: 10.1016/j.polymdegradstab.2008.07.021
- ASTM D 256-10 (2010). "Standard test methods for determining the izod pendulum impact resistance of plastics," ASTM International, West Conshohocken, PA.
- ASTM D 5229 M 14 (2014). "Standard test method for moisture absorption properties and equilibrium conditioning of polymer matrix composite materials," ASTM International, West Conshohocken, PA.
- ASTM D638-10 (2010). "Standard test method for tensile properties of plastics," ASTM International, West Conshohocken, PA.
- ASTM D 790-10 (2010). "Standard test methods for flexural properties of unreinforced and reinforced plastics and electrical insulating materials, test method 1, procedure A," ASTM International, West Conshohocken, PA.
- Balatinecz, J. J., Khavkine, M. I., Law, S., and Kovac, V. (1999). "Properties of polyolefin composites with blends of wood flour and coal ash," in: *Proceedings of the Fifth International Conference on Wood fiber-Plastic Composites*, Forest Products Society, May 26-27, Madison, WI, pp. 235-240.
- Bataille, P., Allard, P., Cousin, P., and Sapiéha, S. (1990). "Interfacial phenomena in cellulose/polyethylene composites," *Polymer Composites* 11(5), 301-304. DOI: 10.1002/pc.750110508
- Boran, S., Kiziltas, A., Kiziltas, E. E., and Gardner, D. J. (2016). "The comparative study of different mixing methods for microcrystalline cellulose/polyethylene composites," *International Polymer Processing* 31(1), 92-103. DOI: 10.3139/217.3156
- Botros, M. (2003). "Development of new generation coupling agents for wood-plastic composites," Equistar Chemicals LP, New Orleans, LA.

- Bourry, D., Godbille, F., Khayat, R. E., Luciani, A., Picot, J., and Utracki, L. A. (1999). "Extensional flow of polymeric dispersions," *Polymer Engineering and Science* 39(6), 1072-1086. DOI:10.1002/pen.11495
- Caulfield, D. F., Jacobson, R. E., Sears, K. D., and Underwood, J. H. (2001). "Fiber reinforced engineering plastics," in: *Proceedings of the Second International Conference on Advanced Engineered Wood Composites*, August 14-16, Maine, ME, pp. 6.
- Chafidz, A., Kaavessina, M., Al-Zahrani, S., and Al-Otaibi, M. N. (2014). "Rheological and mechanical properties of polypropylene/calcium carbonate nanocomposites prepared from masterbatch," *Journal of Thermoplastic Composite Materials* 29(5), 593-622. DOI: 10.1177/0892705714530747
- Cho, J. W., and Paul, D. R. (2001). "Nylon 6 nanocomposites by melt compounding," *Polymer* 42(3), 1083-1094. DOI: 10.1016/S0032-3861(00)00380-3
- Dennis, H. R., Hunter, D. L., Chang, D., Kim, S., White, J. W., Cho, J. W., and Paul, D. R. (2001). "Effect of melt processing conditions on the extent of exfoliation in organoclay-based nanocomposites," *Polymer* 42(23), 9513-9522. DOI: 10.1016/S0032-3861(01)00473-6
- Endo, R., Saito, T., and Isogai, A. (2013). "TEMPO-oxidized cellulose nanofibril/poly(vinyl alcohol) composites drawn fibers," *Polymer* 54(2), 935-941. DOI: 10.1016/j.polymer.2012.12.035
- Etelaaho, P., Nevalainen, K., Suihkonen, R., Vuorinen, J., Hanhi, K., and Jarvela, P. (2009). "Effects of direct melt compounding and masterbatch dilution on the structure and properties of nanoclay-filled polyolefins," *Polymer Engineering and Science* 49(7), 1438-1446. DOI: 10.1002/pen.21270
- Hatzikiriakos, S. G., Rathod, N., and Muliawan, E. B. (2005). "The effect of nanoclays on the processibility of polyolefins," *Polymer Engineering and Science* 45(8), 1098-1107. DOI: 10.1002/pen.20388
- Henriksson, M., Henriksson, G., Berglund, L. A., and Lindström, T. (2007). "An environmentally friendly method for enzyme-assisted preparation of microfibrillated cellulose (MFC) nanofibers," *European Polymer Journal* 43(8), 3434-3441. DOI: 10.1016/j.eurpolymj.2007.05.038
- Herrera-Franco, P. J., and Aguilar-Vega, M. J. (1997). "Effect of fiber treatment on the mechanical properties of LDPE-henequen cellulosic fiber composites," *Journal of Applied Polymer Science* 65(1), 197-207. DOI: 10.1002/(SICI)1097-4628(19970705)65:1<197::AID-APP24>3.0.CO;2-#
- Hitoshi, T., and Akira, A. (2007). "Characterization of 'green' composites reinforced by cellulose nanofibers," *Key Engineering Materials* 334-335, 389-392. DOI: 10.4028/www.scientific.net/KEM.334-335.389
- Ismail, H., Mega, L., and Abdul Khalil, H. P. S. (2001). "Effect of a silane coupling agent on the properties of white rice husk ash-polypropylene/natural rubber composites," *Polymer International* 50(5), 606-611. DOI: 10.1002/pi.673
- JMP Statistical Discovery Software Version 8, Cary, North Carolina, USA.
- Joo, M., Auras, R., and Almenar, E. (2011). "Preparation and characterization of blends made of poly (l-lactic acid) and β -cyclodextrin: Improvement of the blend properties by using a masterbatch," *Carbohydrate Polymers* 86(2), 1022-1030. DOI: 10.1016/j.carbpol.2011.05.058

- Josefsson, G., Berthold, F., and Gamstedt, E. K. (2014). "Stiffness contribution of cellulose nanofibrils to composite materials," *International Journal of Solids and Structures* 51(5), 945-953. DOI:10.1016/j.ijsolstr.2013.11.018
- Khalil, H. P. S., Bhat, A. H., and Yusra, A. F. I. (2012). "Green composites from sustainable cellulose nanofibrils: A review," *Carbohydrate Polymer* 87(2), 963-979. DOI: 10.1016/j.carbpol.2011.08.078
- Kiziltas, A., Gardner, D. J., Han, Y., and Yang, H.-S. (2010). "Determining the mechanical properties of microcrystalline cellulose (MCC)-filled PET-PTT blend composites," *Wood and Fiber Science* 42(2), 165-176.
- Kiziltas, A., Nazari, B., Gardner, D. J., and Bousfield, D. W. (2013). "Polyamide 6-cellulose composites: Effect of cellulose composition on melt rheology and crystallization behavior," *Polymer Engineering and Science* 54(4), 739-746. DOI: 10.1002/pen.23603
- Kiziltas, A., Nazari, B., Kiziltas, E. E., Gardner, D. J., Han, Y., and Rushing, T. S. (2016a). "Cellulose nanofiber-polyethylene nanocomposites modified by polyvinyl alcohol," *Journal of Applied Polymer Science* 133(6), 1-8. DOI: 10.1002/app.42933
- Kiziltas, A., Nazari, B., Erbas Kiziltas, E., Gardner, D. J., Han, Y., and Rushing, T. S. (2016b). "Method to reinforce polylactic acid with cellulose nanofibers via a polyhydroxybutyrate carrier system," *Carbohydrate Polymers* 140, 393-399. DOI: 10.1016/j.carbpol.2015.12.059
- Kvien, I., Tanem, B. S., and Oksman, K. (2005). "Characterization of cellulose whiskers and their nanocomposites by atomic force and electron microscopy," *Biomacromolecules* 6(6), 3160-3165. DOI: 10.1021/bm050479t
- Kvien, I., and Oksman, K. (2007). "Orientation of cellulose nanowhiskers in polyvinyl alcohol," *Applied Physics* A87(4), 641-643. DOI: 10.1007/s00339-007-3882-3
- Lee, S. H., Kim, M. W., Kim, S. H., and Youn, J. R. (2008). "Rheological and electrical properties of polypropylene/MWCNT composites prepared with MWCNT masterbatch chips," *European Polymer Journal* 44(6), 1620-1630. DOI: 10.1016/j.eurpolymj.2008.03.017
- Li, Y.-C., and Chen, G.-H. (2007). "HDPE/expanded graphite nanocomposites prepared via masterbatch process," *Polymer Engineering and Science* 47(6), 882-888. DOI: 10.1002/pen.20772
- Li, J., Ton-That, M. T., Leelapornpisit, W., and Utracki, L. A. (2007). "Melt compounding of polypropylene-based clay nanocomposites," *Polymer Engineering and Science* 47(6), 1447-1458. DOI: 10.1002/pen.20841
- Lopez-Quintanilla, M. L., Sanchez-Valdes, S., Ramos de Valle, L. F., and Medellin-Rodriguez, F. J. (2005). "Effect of some compatibilizing agents on clay dispersion of polypropylene-clay nanocomposites," *Journal of Applied Polymer Science* 100(6), 4748-4756. DOI: 10.1002/app.23262
- Lozano, K., Yang, S., and Jones, R. E. (2004). "Nanofiber toughened polyethylene composites," *Carbon* 42(11), 2329-2331. DOI: 10.1016/j.carbon.2004.03.021
- Luciani, A., and Utracki, L. A. (1996). "The extensional flow mixer, EFM," *International Polymer Processing* 11(4), 299. DOI: 10.3139/217.960299
- Ma, L., Zhang, Y., Meng, Y., Anusonti-Inthra, P., and Wang, S. (2015). "Preparing cellulose nanocrystal/acrylonitrile-butadiene-styrene nanocomposites using the master-batch method," *Carbohydrate Polymers* 125, 352-359. DOI: 10.1016/j.carbpol.2015.02.062

- Mariano, M., Kissi, N. E., and Dufresne, A. (2015). "Melt processing of cellulose nanocrystal reinforced polycarbonate from a masterbatch process," *European Polymer Journal* 69, 208-223. DOI: 10.1016/j.eurpolymj.2015.06.007
- Mathew, A. P., Oksman, K., and Sain, M. (2005). "Mechanical properties of biodegradable composites from poly lactic acid (PLA) and microcrystalline cellulose (MCC)," *Journal of Applied Polymer Science* 97(5), 2014-2025. DOI: 10.1002/app.21779
- Mirabella, F. M., and Bafna, A. (2002). "Determination of the crystallinity of polyethylene/ α -olefin copolymers by thermal analysis: Relationship of the heat of fusion of 100% polyethylene crystal and the density," *Journal of Polymer Science Part B: Polymer Physics* 40(15), 1637-1643. DOI: 10.1002/polb.10228
- Mukherjee, T., Sani, M., Kao, N., Gupta, R. K., Quazi, N., and Bhattacharya, S. (2013). "Improved dispersion of cellulose microcrystals in polylactic acid (PLA) based composites applying surface acetylation," *Chemical Engineering Science* 101, 655-662. DOI: 10.1016/j.ces.2013.07.032
- Nguyen, X. Q., and Utracki, L. A. (1995). "Extensional flow mixer," U.S. Patent 545110619.
- Ozen, E., Kiziltas, A., Erbas Kiziltas, E., and Gardner, D. J. (2013). "Natural fiber blend-nylon 6 composites," *Polymer Composites* 34(4), 544-553. DOI: 10.1002/pc.22463
- Panaitescu, D. M., Notingher, P. V., Ghiurea, M., Ciuprina, F., Paven, H., Iorga, M., and Florea, D. J. (2007a). "Properties of composite materials from polyethylene and cellulose microfibrils," *Journal of Optoelectronics and Advanced Materials* 9(8), 2524-2528.
- Panaitescu, D. M., Donescu, D., Bercu, C., Vuluga, D. M., Iorga, M., and Ghiurea, M. (2007b). "Polymer composites with cellulose microfibrils," *Polymer Engineering and Science* 47(8), 1228-1234. DOI: 10.1002/pen.20803
- Pandey, J. K., Nakagaito, A. N., and Takagi, H. (2013). "Fabrication and applications of cellulose nanoparticle-based polymer composites," *Polymer Engineering and Science* 53(1), 1-8. DOI: 10.1002/pen.23242
- Paunikallio, T., Kasanen, J., Suvanto, M., and Pakkanen, T. T. (2003). "Influence of maleated polypropylene on mechanical properties of composites made of viscose fiber and polypropylene," *Journal of Applied Polymer Science* 87(12), 1895-1900. DOI: 10.1002/app.11919
- Petersson, L., and Oksman, K. (2006). "Biopolymer based nanocomposites: Comparing layered silicates and microcrystalline cellulose as nanoreinforcement," *Composites Science and Technology* 66(13), 2187-2196. DOI: 10.1016/j.compscitech.2005.12.010
- Pöllänen, M., Suvanto, M., and Pakkanen, T. T. (2013). "Cellulose reinforced high density polyethylene composites-morphology, mechanical and thermal expansion properties," *Composites Science and Technology* 76(4), 21-28. DOI: 10.1016/j.compscitech.2012.12.013
- Prashantha, K., Soulestin, J., Lacrampe, M. F., Krawczak, P., Dupin, G., and Claes, M. (2009). "Masterbatch-based multi-walled carbon nanotube filled polypropylene nanocomposites: Assessment of rheological and mechanical properties," *Composites Science and Technology* 69(11-12), 1756-1763. DOI: 10.1016/j.compscitech.2008.10.005
- Ramires, E. C., and Dufresne, A. (2011). "A review of cellulose nanocrystals and nanocomposites," *TAPPI Journal* 10(4), 9-16.
- Rauwendaal, C. (1998). "Polymer mixing: A self-study guide," Hanser, Cincinnati, OH.

- Rauwendaal, C., Rios, A., Osswald, T. A., Gramann, P., Davis, B., Noriega, M. P., and Estrada, O. A. (1999). "Experimental study of a new dispersive mixer," in: *Proceedings from the 57th SPE ANTEC*, May 2-6, Atlanta, GA.
- Sdrobiş, A., Daire, R. N., Totolin, M., Cazacu, G., and Vasile, C. (2012). "Low density polyethylene composites containing cellulose pulp fibers," *Composites Part B: Engineering* 43(4), 1873-1880. DOI: 10.1016/j.compositesb.2012.01.064
- Shao, X., He, L., and Ma, L. (2015). "Study on tensile behavior of natural fiber reinforced pp composites," in: *The 2nd International Forum on Electrical Engineering and Automation (IFEEA 2015)*, December 26-27, pp. 265-268.
- Shumigin, D., Tarasova, E., Krumme, A., and Meier, P. (2011). "Rheological and mechanical properties of poly(lactic) acid/cellulose and LDPE/cellulose composites," *Materials Science* 17(1), 32-37. DOI: 10.5755/j01.ms.17.1.245
- Spoljaric, S., Genovese, A., and Shanks, R. A. (2009). "Polypropylene-microcrystalline cellulose composites with enhanced compatibility and properties," *Composites Part A: Applied Science and Manufacturing* 40(6-7), 791-799. DOI: 10.1016/j.compositesa.2009.03.011
- Šumigin, D., Tarasova, E., Krumme, A., and Viikna, A. (2012). "Influence of cellulose content on thermal properties of poly(lactic) acid/cellulose and low-density polyethylene/cellulose composites," *Proceedings of the Estonian Academy of Sciences* 61(3), 237-244.
- Tajeddin, B., Rahman, R. A., and Abdullah, L. C. (2009). "Mechanical and morphology properties of kenaf cellulose/LDPE biocomposites," *Journal of Agriculture and Environmental Sciences* 5(6), 777-785.
- Ten, E., Bahr, D. F., Li, B., Jiang, L., and Wolcott, M. P. (2012). "Effects of cellulose nanowhiskers on mechanical, dielectric, and rheological properties of poly (3-hydroxybutyrate-co-3-hydroxyvalerate)/cellulose nanowhiskey composites," *Industrial and Engineering Chemistry Research* 51(7), 2941-2951. DOI: 10.1021/ie2023367
- Tokihisa, M., Yakemeto, K., Sakai, T., Utracki, L. A., Sepehr, M., and Simard, L. Y. (2006). "Extensional flow mixer for polymer nanocomposites," *Polymer Engineering and Science* 46(8), 1040-1050. DOI:10.1002/pen.20542
- Treace, M. A., Zhang, W., Moffitt, R. D., and Oberhauser, J. P. (2007). "Twin-screw extrusion of polypropylene-clay nanocomposites: Influence of masterbatch processing, screw rotation mode, and sequence," *Polymer Engineering and Science* 47(6), 898-911. DOI: 10.1002/pen.20774
- Utracki, L. A. (2003). "Polymeric nanocomposites: Compounding and performance," in: *Polymer Nanocomposites*, Boucherville, QC, Canada, October 6-8, pp.1-10.
- Utracki, L. A. (2007). "Polymeric nanocomposites: Compounding and performance," in: *Anais do 9^o Congresso Brasileiro de Polimeros*, October 7, pp.1-10.
- Utracki, L.A., Luciani, A., and Bourry, J. J. (2003). "Extensional flow mixer," US Patent 6550956.
- Volk, N., He, R., and Magniez, K. (2015). "Enhanced homogeneity and interfacial compatibility in melt-extruded cellulose nano-fibers reinforced polyethylene *via* surface adsorption of poly(ethylene glycol)-block-poly(ethylene) amphiphiles," *European Polymer Journal* 72, 270-281. DOI: 10.1016/j.eurpolymj.2015.09.025
- Walther, A., Bjurhager, I., Malho, J.-M., Pere, J., Ruokolainen, J., Berglund, L. A., and Ikkala, O. (2010). "Large-area, lightweight and thick biomimetic composites with

- superior material properties *via* fast, economic, and green pathways,” *Nano Letters* 10(8), 2742-2748. DOI: 10.1021/nl1003224
- Wang, W. and Zloczower, I. M. (2001). “Dispersive and distributive mixing characterization in extrusion equipment,” in: *Antec 2001 Conference Proceedings*, May 6-10, Dallas, TX.
- Yang, H.-S., and Gardner, D. J. (2011). “Morphological characteristics of cellulose nanofibril-filled polypropylene composites,” *Wood and Fiber Science* 43(2), 215-224.
- Yang, H.-S., Gardner, D. J., and Nader, J. W. (2011). “Characteristic impact resistance model analysis of cellulose nanofibril-filled polypropylene composites,” *Composites Part A: Applied Science and Manufacturing* 42(12), 2028-2035. DOI: 10.1016/j.compositesa.2011.09.009
- Yu, Z., Ou, Y., and Feng, Y. (1993). “Effects of coupling agents on the rheological behavior of kaolin filled polyamide 6,” *Chinese Journal of Polymer Science* 11(1), 59-66.

Article submitted: May 25, 2016; July 18, 2016; Revised version received: July 21, 2016;

Accepted: July 22, 2016; Published: August 9, 2016.

DOI: 10.15376/biores.11.4.8178-8199